

Are your MRI contrast agents cost-effective?

Learn more about generic Gadolinium-Based Contrast Agents.



AJNR

This information is current as
of April 9, 2024.

**Susceptibility-Weighted Imaging Improves
the Diagnostic Accuracy of 3T Brain MRI in
the Work-Up of Parkinsonism**

F.J.A. Meijer, A. van Rumund, B.A.C.M. Fassen, I. Titulaer,
M. Aerts, R. Esselink, B.R. Bloem, M.M. Verbeek and B.
Goraj

AJNR Am J Neuroradiol 2015, 36 (3) 454-460

doi: <https://doi.org/10.3174/ajnr.A4140>

<http://www.ajnr.org/content/36/3/454>

Susceptibility-Weighted Imaging Improves the Diagnostic Accuracy of 3T Brain MRI in the Work-Up of Parkinsonism

F.J.A. Meijer, A. van Rumund, B.A.C.M. Fasen, I. Titulaer, M. Aerts, R. Esselink, B.R. Bloem, M.M. Verbeek, and B. Goraj



ABSTRACT

BACKGROUND AND PURPOSE: The differentiation between Parkinson disease and atypical parkinsonian syndromes can be challenging in clinical practice, especially in early disease stages. Brain MR imaging can help to increase certainty about the diagnosis. Our goal was to evaluate the added value of SWI in relation to conventional 3T brain MR imaging for the diagnostic work-up of early-stage parkinsonism.

MATERIALS AND METHODS: This was a prospective observational cohort study of 65 patients presenting with parkinsonism but with an uncertain initial clinical diagnosis. At baseline, 3T brain MR imaging with conventional and SWI sequences was performed. After clinical follow-up, probable diagnoses could be made in 56 patients, 38 patients diagnosed with Parkinson disease and 18 patients diagnosed with atypical parkinsonian syndromes, including 12 patients diagnosed with multiple system atrophy–parkinsonian form. In addition, 13 healthy controls were evaluated with SWI. Abnormal findings on conventional brain MR imaging were grouped into disease-specific scores. SWI was analyzed by a region-of-interest method of different brain structures. One-way ANOVA was performed to analyze group differences. Receiver operating characteristic analyses were performed to evaluate the diagnostic accuracy of conventional brain MR imaging separately and combined with SWI.

RESULTS: Disease-specific scores of conventional brain MR imaging had a high specificity for atypical parkinsonian syndromes (80%–90%), but sensitivity was limited (50%–80%). The mean SWI signal intensity of the putamen was significantly lower for multiple system atrophy–parkinsonian form than for Parkinson disease and controls ($P < .001$). The presence of severe dorsal putaminal hypointensity improved the accuracy of brain MR imaging: The area under the curve was increased from 0.75 to 0.83 for identifying multiple system atrophy–parkinsonian form, and it was increased from 0.76 to 0.82 for identifying atypical parkinsonian syndromes as a group.

CONCLUSIONS: SWI improves the diagnostic accuracy of 3T brain MR imaging in the work-up of parkinsonism by identifying severe putaminal hypointensity as a sign indicative of multiple system atrophy–parkinsonian form.

ABBREVIATIONS: AP = atypical parkinsonian syndromes; AUC = area under the curve; CBS = corticobasal syndrome; DLB = dementia with Lewy bodies; HC = healthy controls; MSA = multiple system atrophy; MSA-P = multiple system atrophy–parkinsonian form; PD = Parkinson disease; PSP = progressive supranuclear palsy; ROC = receiver operating characteristic; SI = signal intensity

In clinical practice, the differentiation between Parkinson disease (PD) and atypical parkinsonian syndromes (AP), such as multiple system atrophy (MSA), progressive supranuclear palsy (PSP), corticobasal syndrome (CBS), and dementia with Lewy bodies (DLB), can be challenging. For adequate patient counsel-

ing and treatment planning, it is important to make the correct diagnosis at an early disease stage. Ancillary investigations such as brain MR imaging can be performed to increase certainty about the diagnosis. In the diagnostic work-up of parkinsonism, performing brain MR imaging is advised because it can support the diagnosis of AP or vascular parkinsonism.¹ Also, brain MR imaging can demonstrate other more rare causes of parkinsonism such as normal pressure hydrocephalus or multiple sclerosis.


Conventional brain MR imaging findings, including those of T1, T2, T2 FLAIR, and proton-attenuation sequences, are usually normal in PD or will show age-related changes.² Atrophy or


Received June 16, 2014; accepted after revision August 10.

From the Departments of Radiology and Nuclear Medicine (F.J.A.M., B.A.C.M.F., B.G.) and Laboratory Medicine (M.M.V.), and Department of Neurology (A.v.R., I.T., M.A., R.E., B.R.B., M.M.V.), Donders Institute for Brain, Cognition and Behavior, Radboud University Nijmegen Medical Center, Nijmegen, the Netherlands; and Department of Diagnostic Imaging (B.G.), Medical Center of Postgraduate Education, Warsaw, Poland.

This work was supported by Stichting Internationaal Parkinson Fonds and het Van Alkemade Keuls Fonds.

Please address correspondence to Frederick J.A. Meijer, MD, Radboud University Nijmegen Medical Center, Department of Radiology and Nuclear Medicine, Postbus 9101, 6500 HB Nijmegen, the Netherlands; e-mail: Anton.Meijer@radboudumc.nl

 Indicates article with supplemental on-line tables.

 Indicates article with supplemental on-line photo.

<http://dx.doi.org/10.3174/ajnr.A4140>

Table 1: MRI scanning protocol

Sequence	TR (ms)	TE (ms)	Flip Angle	Voxel Size (mm)	No. and Direction of Sections	iPAT Factor	Acquisition Time (min:sec)
T2 TSE	5830	120	120°	0.6 × 0.6 × 3	48 Axial	—	3:43
T1 MPRAGE	2300	4.71	12°	1 × 1 × 1	192 Sagittal	2	5:47
T2 FLAIR	9000	86	150°	0.7 × 0.6 × 5	28 Axial	2	2:44
Proton-attenuation	2000	20	90°	0.9 × 0.9 × 3	48 Axial	—	7:16
DWI-EPI ($b=0$ and $b=1000$)	3900	89	90°	1.3 × 1.3 × 5	48 Axial	2	2:10
SWI gradient-echo	29	20	15°	0.6 × 0.6 × 3	48 Axial	2	4:42

Note:—iPAT indicates integrated parallel acquisition technique.

signal-intensity (SI) changes of specific regions of the brain identified on brain MR imaging can have high specificity for the different forms of AP. Examples include putaminal or pontine atrophy in MSA and midbrain atrophy (hummingbird sign) in PSP. The sensitivity of brain MR imaging for AP is generally limited, especially in early disease stages.^{3–5}

New MR imaging techniques have become available for clinical practice in recent years, including susceptibility-weighted imaging. SWI is sensitive to magnetic susceptibility differences in tissues such as blood, calcification, and iron deposition. Because SWI makes use of both magnitude and phase information during image acquisition, it is superior in detecting brain susceptibility changes in comparison with T2* gradient-echo sequences.^{6,7} SWI is emerging as a useful technique in a wide variety of intracranial pathologies, including neurodegenerative diseases.⁸ In parkinsonian syndromes, there are different patterns of abnormal brain iron metabolism in PD and AP. Examples include increased iron accumulation in the substantia nigra in PD and increased striatal iron content in MSA.⁹ These patterns of abnormal brain iron content should be differentiated from physiologic age-related iron accumulation.^{10,11} Also, there still is debate about whether disturbances in iron levels in PD constitute representation of the primary pathologic process or are a secondary consequence.¹² This debate is highly relevant for SWI because it influences whether abnormal iron content in brain structures can be identified in early-stage PD or AP. Initial reports on SWI in parkinsonism indicate that SWI may provide new diagnostic markers for clinical use.^{13,14}

The goal of our study was to evaluate whether SWI is of added value in relation to conventional 3T brain MR imaging in the diagnostic work-up of early-stage parkinsonism.

MATERIALS AND METHODS

Study Group

We performed a prospective observational study in 65 patients presenting with parkinsonism with a disease duration of <3 years, with major uncertainty of the underlying diagnosis on inclusion. Patients were consecutively recruited at our outpatient movement disorder clinic during 2010–2012. Study inclusion criteria were clinical signs and symptoms of parkinsonism (hypokinetic-rigid syndrome) with an uncertain clinical diagnosis and disease duration of <3 years. Exclusion criteria were age younger than 18 years, prior brain surgery, the presence of another neurodegenerative disorder, and unstable comorbidity. The medical ethics committee of our hospital approved the study, and all participants gave written informed consent. For the sake of the SWI analyses, we also enrolled 13 age- and sex-matched healthy controls, who were scanned with the SWI sequence.

Study Design

Patients had a clinical assessment at baseline by standardized history taking and neurologic examination by an experienced physician (M.A., A.v.R.). Cardiovascular risk factors, activities in daily living, medication use, disease onset, clinical signs, most affected body site, and balance and fear of falling were assessed. Clinical neurologic scores were applied, including the Non-Motor Symptoms Scale¹⁵ and the Mini-Mental State Examination¹⁶ to evaluate global cognitive status and the Unified Parkinson's Disease Rating Scale¹⁷ and the Hoehn and Yahr Staging Scale¹⁸ to evaluate motor function.

At baseline, all patients underwent brain MR imaging. After clinical follow-up, final diagnoses could be made by 2 experienced clinicians (A.v.R., R.E.). These diagnoses were made according to international diagnostic criteria^{19–24} based on neurologic signs that developed during the course of the disease (as identified during repeat neurologic examinations), rate of disease progression, and treatment response. Our primary interest was to evaluate the added value of SWI in relation to conventional 3T brain MR imaging performed in the early disease stage in differentiating PD and the various forms of AP.

Brain MR Imaging Protocol

At baseline, all patients underwent 3T MR imaging of the brain (Magnetom Trio; Siemens, Erlangen, Germany). The scanning protocol included 3D T1 MPRAGE, T2 TSE, T2 FLAIR, proton-attenuation, and DWI sequences. The SWI sequence was a 3D gradient echo acquisition; magnitude and phase images were obtained in the axial plane. Details of the scanning protocol are provided in Table 1. In addition to our patient cohort, 13 age-matched healthy controls (HC) were scanned with the SWI sequence.

Imaging Analysis

Two neuroradiologists (F.J.A.M. and B.G.) evaluated conventional brain MR imaging studies in a standardized manner, blinded to clinical information. First, abnormalities that have been validated for the evaluation of parkinsonian syndromes were scored.^{3–5,25} Second, selected abnormalities were grouped in a score typical for a given disease. Atrophy and T2 hypointensity changes of the putamen, pontine atrophy, hot cross bun sign, cerebellar atrophy, and T2 hyperintense signal changes of the middle cerebellar peduncle were combined in the “MSA” score. Midbrain atrophy, hummingbird sign, and a reduced AP midbrain diameter of <14 mm were scored and combined in the “PSP” score. Cortical atrophy and third and lateral ventricle dilation were scored and combined in the “Atrophy” score as a manifestation of CBS or DLB. The “MSA,” “PSP,” and “Atrophy” scores combined resulted in the “Sum” score, which was used to

evaluate AP as a group. Several thresholds (eg, the presence of 1, 2, 3, or 4 abnormalities) were applied to these scores to evaluate the diagnostic accuracy of conventional brain MR imaging for the different forms of AP. Furthermore, white matter changes and the presence of infarction were scored.

The region-of-interest method was used to evaluate the SWI sequences on an Impax workstation, Version 6.5.3 (Agfa-Gevaert, Mortsel, Belgium). A 4.9-mm² circular region of interest was placed bilaterally in the following structures: caudate nucleus, putamen (anterior and posterior), red nucleus, substantia nigra (anterior and posterior), globus pallidus, thalamus, pulvinar thalamus, and dentate nucleus. The region of interest was placed in the most hypointense part of the brain structure, avoiding vessels and not including the edges of the structure. Additionally, the signal intensity of CSF was measured by region-of-interest placement in the fourth ventricle. SWI signal intensity of the different brain structures was normalized to CSF with a signal intensity of 200, to correct for inconsistencies in the reference standard. Two readers (F.J.A.M. and B.A.C.M.F.), blinded to the clinical symptoms and diagnoses, performed the region-of-interest analysis of the SWI sequences. One reader (B.A.C.M.F.) performed the region-of-interest analysis twice to evaluate intrarater variability.

Increased susceptibility is defined here as decreased SWI signal intensity. On the basis of the mean signal intensity values obtained, the hypointensity was graded according the criteria proposed by Gupta et al (Fig 1)¹³:

- Grade 0: SI similar to CSF intensity (SI > 200)
- Grade 1: mild hypointensity (SI > 150 but <200)
- Grade 2: moderate hypointensity (SI > 75 but <150)
- Grade 3: severe hypointensity (SI < 75).

Statistical Analyses

The diagnostic accuracy of the conventional brain MR imaging “MSA,” “PSP,” “Atrophy,” and “Sum” scores to identify the different forms of AP was calculated. Cohen κ coefficient was used to evaluate interrater variability of abnormalities scored on conventional brain MR imaging. For SWI, both intra- and interrater agreement was evaluated. Agreement was graded as the following: $\kappa < 0.20$, poor agreement; 0.21–0.40, fair agreement; 0.41–0.60, moderate agreement; 0.61–0.80, good agreement; >0.80 , perfect agreement.

The mean SWI signal intensity of the brain structures was calculated for each diagnosis, and 1-way ANOVA, corrected for multiple comparisons with a Bonferroni correction, was performed to analyze group differences. A P value $< .05$ was considered statistically significant for disease-specific SWI changes.

Finally, the area under the curve (AUC) of the receiver operating characteristic (ROC) was used to evaluate the discriminative power of conventional brain MR imaging alone and in combination with selected SWI measures.

All statistical analyses were performed with SPSS (Version 20; IBM, Armonk, New York).

RESULTS

Study Group

Patients had a mean follow-up of 24.8 ± 12 months. Of the 65 patients, 9 were excluded for the following reasons: brain MR

imaging with severe artifacts ($n = 2$), uncertain diagnosis ($n = 4$), diagnosis other than PD or AP ($n = 1$), and diagnosis of vascular parkinsonism ($n = 2$).

Of the remaining 56 patients, 38 patients were diagnosed with PD, and 18 patients, with AP (12 with multiple system atrophy–parkinsonian form [MSA-P], 3 with PSP, and 3 with DLB). Demographic data of the study population and control group are shown in Table 2.

Conventional Brain MR Imaging Results

Abnormalities scored on conventional brain MR imaging are summarized in On-line Table 1. Overall there was good interrater agreement for the abnormalities scored on brain MR imaging with perfect interrater agreement ($\kappa > 0.8$) for atrophy and signal-intensity changes of the putamen and midbrain. Pontine and cerebellar atrophy and T2 hyperintensity changes of the middle cerebellar peduncle showed moderate interrater agreement ($\kappa = 0.47$ – 0.54). There was poor agreement for the putaminal rim sign. The putaminal rim sign proved not to be indicative of MSA on 3T MR imaging (sensitivity, 42%; specificity, 48% for MSA), which is in line with a previous report.²⁶ Therefore, we did not include the putaminal rim sign in further analyses.

The diagnostic accuracy of conventional brain MR imaging abnormalities combined in group scores to identify the different forms of AP is shown in Table 3. Sensitivity and specificity can be influenced by choosing a threshold—eg, the presence of at least 1 abnormality for the “MSA” score to identify MSA-P results in 83% sensitivity with 66% specificity, while the presence of at least 2 abnormalities results in 25% sensitivity with 93% specificity. The presence of at least 2 abnormalities on conventional brain MR imaging has reasonable sensitivity (78%) and specificity (76%) to identify AP as a group. The specificity for AP can be increased (89%) by considering the presence of at least 4 abnormalities for the diagnosis of AP, though at the cost of sensitivity (50%).

MR Imaging SWI Analysis

Significantly lower mean SWI signal intensity of the putamen was found in MSA-P, in comparison with PD and HC (On-line Table 2). This finding was consistent for both sides and the anterior and posterior parts of the putamen (all regions, $P < .001$ for MSA-P versus PD, for both readers). Signal intensity of the posterior putamen was compared with that of the anterior part. The distribution of putaminal signal intensities for the different disease groups demonstrated that grade 3 hypointensity changes of the posterior putamen discriminated MSA-P from the other groups (boxplots in On-line Fig 1). For the anterior putamen, the presence of grade 2 or 3 hypointensity changes discriminated MSA-P from the other groups. There was good intrarater ($\kappa = 0.76$) and interrater ($\kappa = 0.80$) agreement for the putaminal SWI hypointensity grading.

Lower mean SWI signal intensity of the caudate nucleus was seen in MSA-P; the difference in signal intensity was statistically significant on the left side in comparison to PD. Caudate nucleus signal intensity (mean grade 1 hypointensity) was not as low as that for the putamen. In PSP, significantly decreased mean SWI

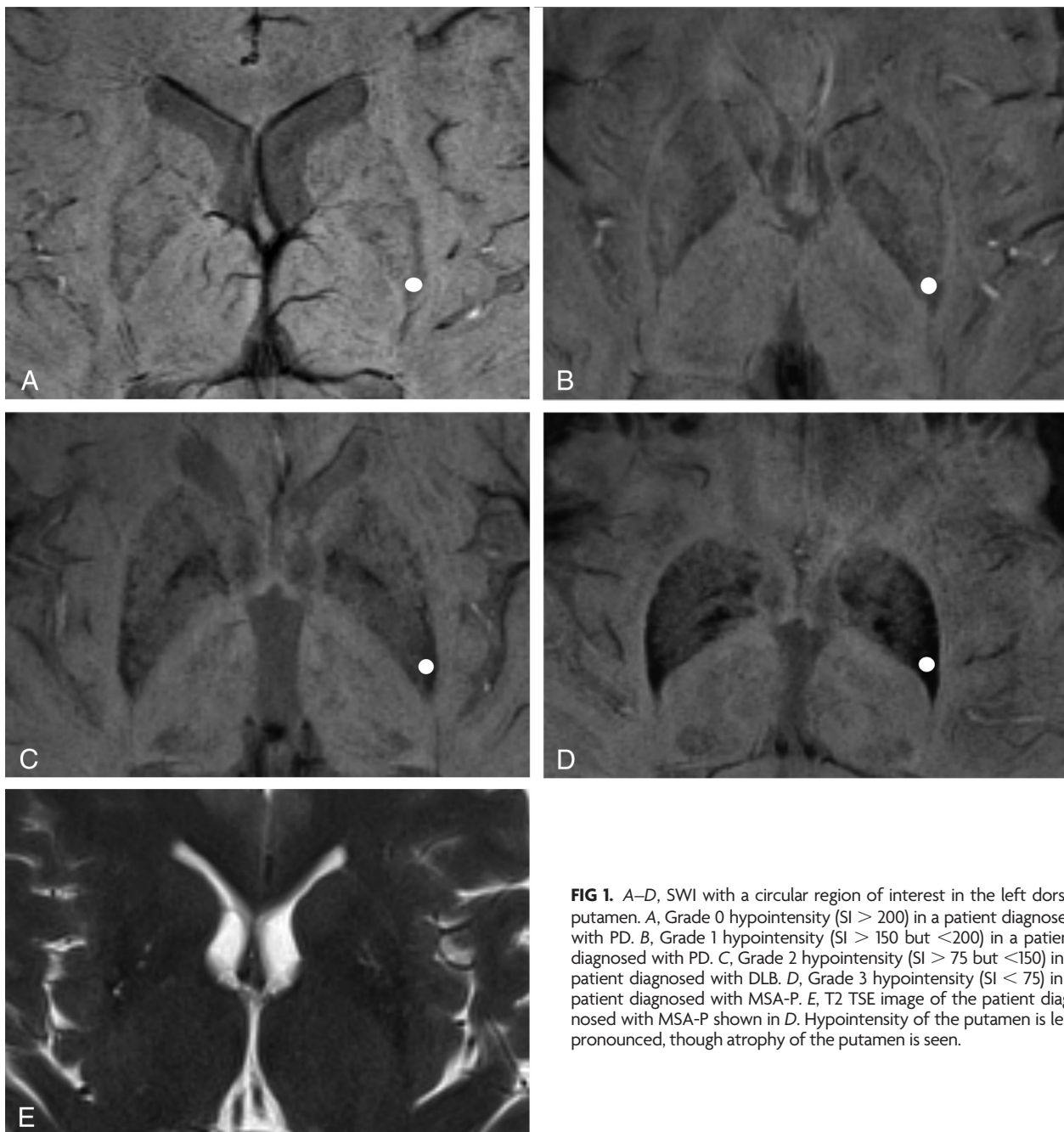


FIG 1. A–D, SWI with a circular region of interest in the left dorsal putamen. A, Grade 0 hypointensity (SI > 200) in a patient diagnosed with PD. B, Grade 1 hypointensity (SI > 150 but < 200) in a patient diagnosed with PD. C, Grade 2 hypointensity (SI > 75 but < 150) in a patient diagnosed with DLB. D, Grade 3 hypointensity (SI < 75) in a patient diagnosed with MSA-P. E, T2 TSE image of the patient diagnosed with MSA-P shown in D. Hypointensity of the putamen is less pronounced, though atrophy of the putamen is seen.

Table 2: Patient characteristics^a

	PD (n = 38)	AP (n = 18)	MSA-P (n = 12)	PSP (n = 3)	DLB (n = 3)	HC (n = 13)
Age (yr)	61 (9)	65 (8)	63 (9)	67 (5)	69 (3)	67 (7)
Sex (M/F)	23:15	9:9	6:6	1:2	2:1	9:4
Disease duration (mo)	19.1 (14)	15.2 (12)	15.5 (11)	23.0 (20)	6.7 (7)	—
UPDRS-III	32.1 (12)	45.2 (11)	45.5 (12)	47.5 (13)	42.7 (11)	—
H&Y	1.7 (0.7)	2.6 (0.9)	2.6 (1.0)	3.0 (0)	2.3 (0.6)	—
MMSE	28.5 (1.6)	28.1 (1.6)	28.4 (1.4)	28.7 (0.6)	26.0 (1.0)	—

Note:—UPDRS-III indicates Unified Parkinson's Disease Rating Scale-III; H&Y, Hoehn and Yahr Staging Scale; MMSE, Mini-Mental State Examination.

^a Data are mean or number (SD).

signal intensities (grade 2 hypointensity) of the red and dentate nuclei on the left side were found in comparison with those in PD and HC.

In comparison with the different forms of AP and HC, no

statistically significant SWI signal-intensity changes of the different brain structures were found for PD.

On the basis of the findings above, SWI hypointensity grading of the putamen was used for further analyses in eval-

Table 3: Frequency (%) of positive results^a

	PD (n = 38)	MSA-P (n = 12)	PSP (n = 3)	DLB (n = 3)	Sensitivity/Specificity	κ (Interrater)
"MSA" score, threshold 1	11 (29)	10 (83)	1 (33)	3 (100)	83%/66% for MSA	0.64
"MSA" score, threshold 2	2 (5)	3 (25)	0 (0)	1 (33)	25%/93% for MSA	0.59
"PSP" score, threshold 1	0 (0)	1 (8)	3 (100)	0 (0)	100%/98% for PSP	0.88
"Atrophy" score, threshold 2	7 (18)	4 (33)	3 (100)	2 (67)	67%/74% for DLB	0.86
"Sum" score, threshold 2	9 (24)	8 (67)	3 (100)	3 (100)	78%/76% for AP	0.75
"Sum" score, threshold 3	8 (21)	5 (42)	3 (100)	2 (67)	56%/79% for AP	0.80
"Sum" score, threshold 4	4 (11)	4 (33)	3 (100)	2 (67)	50%/89% for AP	0.64

^a Threshold criteria defined as the presence of either 1, 2, 3, or 4 abnormalities on conventional brain MRI for the different scores.

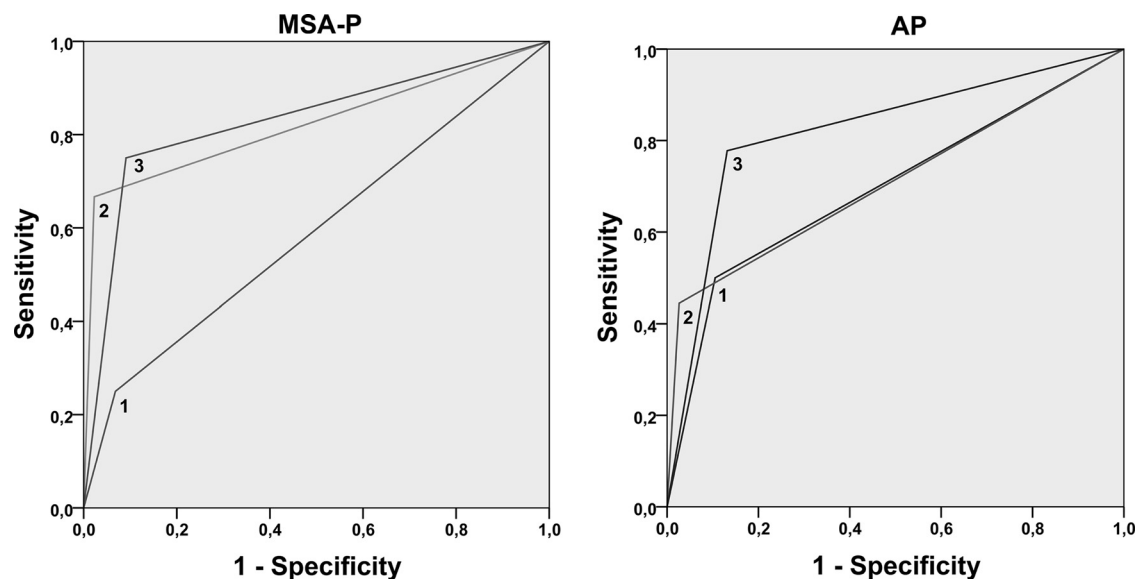


FIG 2. ROC curves to evaluate diagnostic accuracy. Point 1 indicates the brain MR imaging "MSA" score to identify MSA-P, threshold 2 abnormalities (left figure), and the MR imaging "Sum" score to identify AP as a group, threshold 4 abnormalities (right figure). Point 2 is the grade 3 SWI hypointensity of the dorsal putamen. Point 3 indicates points 1 and 2 combined. SWI increases sensitivity with preservation of high specificity.

uating the diagnostic accuracy of brain MR imaging and SWI.

Evaluation of Diagnostic Accuracy

SWI grade 3 hypointensity of the posterior putamen proved to be superior to grade 2 or 3 hypointensity of the anterior putamen for identifying MSA-P (AUC, 0.82 versus 0.69). The results of the ROC analyses to evaluate the diagnostic accuracy of conventional brain MR imaging alone and in combination with SWI grade 3 hypointensities of the putamen are shown in Fig 2 and On-line Tables 3 and 4.

Diagnosis of MSA-P

Conventional brain MR imaging "MSA" score, with a threshold of at least 2 abnormalities present, results in an AUC of 0.59 (confidence interval, 0.40–0.79) to identify MSA-P. Threshold 1 results in an AUC of 0.75 (confidence interval, 0.60–0.90). The AUC is increased to 0.83 (confidence interval, 0.68–0.98) when combining the conventional brain MR imaging threshold 2 with the presence of SWI grade 3 hypointensity of the posterior putamen. This increase in AUC is explained by a significant improvement in sensitivity (25%–75%) with preservation of high specificity (91%).

Diagnosis of AP

The conventional brain MR imaging "Sum" score, when at least 2 abnormalities are present, results in the highest AUC of 0.76 (confidence interval, 0.62–0.90) to identify AP as a group. The AUC can be

increased to 0.82 (confidence interval, 0.69–0.95) when combining the conventional brain MR imaging "Sum" score with at least 4 abnormalities present with SWI grade 3 hypointensity of the posterior putamen. The improved diagnostic accuracy results from improved sensitivity (50%–78%) with preservation of high specificity (87%).

DISCUSSION

Unlike previous studies, we prospectively evaluated both conventional brain MR imaging and SWI in patients presenting with parkinsonism with an initial uncertain diagnosis, in whom increase of certainty about the diagnosis is of the most clinical relevance. In our study population, the ability of conventional 3T brain MR imaging to differentiate PD and the different atypical parkinsonian syndromes was limited and depended on defined diagnostic criteria. When combined with SWI, the diagnostic accuracy was improved, mainly by identifying severe hypointensity of the putamen, which is indicative of MSA-P.

Patterns of normal age-related iron content of the different brain structures have been described in literature, including age-related increase in iron content of the putamen.^{27,28} Because we included a group of age-matched healthy controls, it is more likely that the increased putaminal susceptibility in MSA-P found in our study reflects pathologic mineralization rather than a result of aging.

Increased iron concentrations and decreased signal intensity on T2 spin-echo and T2* gradient echo-weighted sequences of

the putamen, but also of the caudate nucleus, have been reported previously in MSA.^{9,29-33} Susceptibility changes of the putamen are depicted more accurately by SWI than by a T2 spin-echo sequence (Fig 1D, -E). With regard to SWI, decreased signal intensity of the putamen in MSA has been described,¹⁴ though not confirmed by others.³⁴ Gupta et al¹³ found higher putaminal SWI hypointensity scores in MSA-P, though this difference was not statistically significant. Wang et al¹⁴ found increased iron deposition in the putamen in MSA-P, as we did, and reported that the lower inner region of the putamen was the most valuable subregion in differentiating MSA-P from PD, while in our study, this finding is valid for the posterior part of the putamen.

Gupta et al¹³ reported higher hypointensity scores of the putamen and red nucleus in PSP, in comparison with PD and MSA. In our study population, the SWI signal intensities of the red nucleus and dentate nucleus were lower in PSP compared with PD, with statistical significance on the left side. This finding is in line with observed neuropathologic changes of these structures in PSP.³⁵ SWI hypointensity changes of these nuclei could therefore possibly provide a new diagnostic marker for PSP. Increased iron content in the substantia nigra and putamen have been reported in PSP mainly in advanced disease stages, but not in the amount seen in MSA.⁹ According to the literature, there is little evidence of increased brain iron levels in DLB, but possibly the substantia nigra is affected.⁹

SWI signal intensity is influenced by many factors besides iron content of brain structures, including acquisition parameters and magnetic field strength but also by spatial position and reconstruction algorithms (which differ across MR imaging vendors). For reproducibility of quantitative analyses, it is important to apply a normalization technique. Our study population was scanned by using a 3T MR imaging scanner, while others used a 1.5T scanner.^{13,14} It is likely that differences in magnetic field strengths could partly explain discrepancies in study results because a 3T MR imaging scanner is more sensitive to susceptibility changes than a 1.5T scanner.^{36,37}

On the basis of their 3T MR imaging SWI study, Haller et al³⁴ found increased susceptibility in the thalamus and left substantia nigra in PD, and they reported good discrimination between PD and AP by using a support-vector analysis. Unfortunately, they did not include a healthy control group to evaluate whether the observed increased susceptibility in the substantia nigra and thalamus is PD-specific. In our study population, we did not observe changes in the susceptibility of the substantia nigra or other brain structures in PD in comparison with patients with AP or matched healthy control subjects. A possible explanation could be that our patients with PD were scanned in earlier disease stages. In previous studies however, no clear evidence was found of substantia nigra iron content being related to disease duration.^{38,39} In recent in vivo and postmortem SWI studies, a subregion of the substantia nigra pars compacta, called nigrosome 1, was reported to be absent in PD.^{40,41} A "swallow tail" appearance of the healthy nigrosome 1 and its absence in PD have recently been evaluated in a case control study with observed good discrimination between patients with PD and HC.⁴² It is not known whether the absence of nigrosome 1 on SWI could discriminate PD from AP.

There are some limitations to our study. First, our study population was relatively small, especially for the AP group, and conclusions were mainly based on a comparison among PD, MSA-P,

and HC. Therefore, definite conclusions regarding other forms of AP cannot be made. On the other hand, the prevalence of less frequent parkinsonian syndromes in our cohort does reflect clinical practice and draws attention to the need for ancillary investigations aiming to improve certainty about the diagnosis in a patient presenting with parkinsonism. The subjects of our study were patients with parkinsonism and uncertain clinical diagnosis, which could explain the relatively low frequency of the different forms of atypical parkinsonism in our study population.

The small number of patients diagnosed with PSP could explain why the lower signal intensity values of the red nucleus and dentate nucleus were only statistically significant unilaterally. Whether the SWI sequence is of added value for the diagnosis of PSP, CBS, DLB, or other forms of AP not included in our study, such as multiple system atrophy—cerebellar form and CBS, remains to be determined. In vascular parkinsonism, SWI could be of additional value to identify microbleeds as a sign of microangiopathy, but this possibility was beyond the scope of our study.

Second, we did not have postmortem confirmation of the diagnoses; therefore, we cannot fully rule out misdiagnosis in our study population. The diagnoses were made by a movement-disorder specialist on the basis of accepted diagnostic criteria, after a mean follow-up of 24.5 months. This approach proved to yield high accuracy (>90%) as shown in a previous clinical-pathologic study.⁴³

Third, because there are only a few studies available in which SWI has been evaluated in parkinsonism, validation of diagnostic criteria is crucial for optimal use in daily clinical practice. This validation also applies to the conventional brain sequences because diagnostic criteria have not been standardized. Because abnormalities on brain MR imaging differ for the various forms of AP, disease-specific diagnostic criteria give a more accurate estimation of the diagnostic accuracy of brain MR imaging rather than grouping all the forms of AP together. Standardization of the scanning protocol, with the magnetic field strength of the MR imaging study taken into account, and postprocessing methods is necessary for validation of diagnostic criteria.

Other advanced MR imaging techniques, including diffusion (tensor) imaging, magnetization transfer imaging, and functional MR imaging could possibly provide new diagnostic markers for PD or AP. In future clinical cohort studies, it would be interesting to study the diagnostic value of SWI in relation to these advanced imaging techniques.

CONCLUSIONS

SWI proved a useful sequence in addition to conventional 3T brain MR imaging in the diagnostic work-up of early-stage parkinsonism. SWI improves the diagnostic accuracy of 3T brain MR imaging by detecting severe hypointensity of the putamen as a sign indicative of MSA-P.

Disclosures: Bastiaan R. Bloem—UNRELATED: Board Membership: ZonMw*; Consultancy: UCB,* Glaxo-Smith-Kline,* Danone*; Grants/Grants Pending: ZonMw*, Michael J. Fox Foundation,* Davis Phinney Foundation*; Payment for Lectures (including service on Speakers Bureaus): AbbVie*; OTHER RELATIONSHIPS: B.R. Bloem was an Editorial Board member of *Movement Disorders* (earlier) and Associate Editor for the *Journal of Parkinson's Disease* (currently), and received funds from the Alkemade Keuls fund, the Michael J. Fox Foundation, the Netherlands Organization of Scientific Research, the Prinses Beatrix Foundation, and the Stichting Internationaal Parkinson Fonds. Marcel M. Verbeek—RELATED: Grant: Stichting Internationaal Parkinson Fonds*; OTHER RELATIONSHIPS: Associate Editor of the *Journal of Alzheimer's Disease*.

mer's Disease; Editorial Board member, *International Journal of Molecular Epidemiology and Genetics*; Editorial Board member, *American Journal of Neurodegenerative Diseases*; Editorial Board member, *Molecular Neurodegeneration*; received funding from Internationale Stichting Alzheimer Onderzoek; Joint Programming in Neurodegenerative Disease, Alzheimer's Drug Discovery Foundation. *Money paid to the institution.

REFERENCES

- Berardelli A, Wenning GK, Antonini A, et al. EFNS/MDS-ES/ENS [corrected] recommendations for the diagnosis of Parkinson's disease. *Eur J Neurol* 2013;20:16–34
- Brooks DJ. Morphological and functional imaging studies on the diagnosis and progression of Parkinson's disease. *J Neurol* 2000;247(suppl 2):11–18
- Schrag A, Good CD, Miskiel K, et al. Differentiation of atypical parkinsonian syndromes with conventional brain MRI. *Neurology* 2000;54:697–702
- Mahlknecht P, Hotter A, Hussl A, et al. Significance of MRI in diagnosis and differential diagnosis of Parkinson's disease. *Neurodegener Dis* 2010;7:300–18
- Meijer FJ, Aerts MB, Abdo WF, et al. Contribution of conventional brain MRI to the differential diagnosis of parkinsonism: a 3-year prospective follow-up study. *J Neurol* 2012;259:929–35
- Haacke EM, Xu Y, Cheng YC, et al. Susceptibility weighted imaging (SWI). *Magn Reson Med* 2004;52:612–18
- Haacke EM, Cheng NY, House MJ, et al. Imaging iron stores in the brain using magnetic resonance imaging. *Magn Reson Imaging* 2005;23:1–25
- Sehgal V, Delproposto Z, Haacke EM, et al. Clinical applications of neuroimaging with susceptibility-weighted imaging. *J Magn Reson Imaging* 2005;22:439–50
- Berg D, Hochstrasser H. Iron metabolism in Parkinsonian syndromes. *Mov Disord* 2006;21:1299–310
- Haacke EM, Ayaz M, Khan A, et al. Establishing a baseline phase behavior in magnetic resonance imaging to determine normal vs. abnormal iron content in brain. *J Magn Reson Imaging* 2007;26:256–64
- Harder SL, Hopp KM, Ward H, et al. Mineralization of the deep gray matter with age: a retrospective review with susceptibility-weighted MR imaging. *AJNR Am J Neuroradiol* 2008;29:176–83
- Friedman A, Galazka-Friedman J, Koziorowski D. Iron as a cause of Parkinson disease: a myth or a well-established hypothesis? *Parkinsonism Relat Disord* 2009;15(suppl 3):212–14
- Gupta D, Saini J, Kesavadas C, et al. Utility of susceptibility-weighted MRI in differentiating Parkinson's disease and atypical parkinsonian syndromes. *Neuroradiology* 2010;52:1087–94
- Wang Y, Butros SC, Shuai X, et al. Different iron-deposition patterns of multiple system atrophy with predominant parkinsonism and idiopathic Parkinson diseases demonstrated by phase-corrected susceptibility-weighted imaging. *AJNR Am J Neuroradiol* 2012;33:266–73
- Chaudhuri KR, Martinez-Martin P. Quantitation of non-motor symptoms in Parkinson's disease. *Eur J Neurol* 2008;15(suppl 2):2–7
- Folstein MF, Robins LN, Helzer JE. The Mini-Mental State Examination. *Arch Gen Psychiatry* 1983;40:812
- Fahn S, Elton RL. Unified Parkinson's Disease Rating Scale. In: Fahn S, Marsden CD, Calne D, eds. *Recent Developments in Parkinson's Disease*. Vol 2. Florham Park: MacMillan Healthcare Information; 1987:153–63
- Hoehn MM, Yahr MD. Parkinsonism: onset, progression, and mortality. *Neurology* 1967;17:427–42
- Gelb DJ, Oliver E, Gilman S. Diagnostic criteria for Parkinson disease. *Arch Neurol* 1999;56:33–39
- Gilman S, Wenning GK, Low PA, et al. Second consensus statement on the diagnosis of multiple system atrophy. *Neurology* 2008;71:670–76
- Litvan I, Agid Y, Calne D, et al. Clinical research criteria for the diagnosis of progressive supranuclear palsy (Steele-Richardson-Olszewski syndrome): report of the NINDS-SPSP international workshop. *Neurology* 1996;47:1–9
- McKeith IG, Dickson DW, Lowe J, et al. Consortium on DLB: diagnosis and management of dementia with Lewy bodies: third report of the DLB Consortium. *Neurology* 2005;65:1863–72
- Boeve BF, Lang AE, Litvan I. Corticobasal degeneration and its relationship to progressive supranuclear palsy and frontotemporal dementia. *Ann Neurol* 2003;54(suppl 5):15–19
- Zijlmans JC, Daniel SE, Hughes AJ, et al. Clinicopathological investigation of vascular parkinsonism, including clinical criteria for diagnosis. *Mov Disord* 2004;19:630–40
- Yekhelef F, Ballan G, Macia F, et al. Routine MRI for the differential diagnosis of Parkinson's disease, MSA, PSP, and CBD. *J Neural Transm* 2003;110:151–69
- Lee WH, Lee CC, Shyu WC, et al. Hyperintense putaminal rim sign is not a hallmark of multiple system atrophy at 3T. *AJNR Am J Neuroradiol* 2005;26:2238–42
- Hallgren B, and Sourander P. The effect of age on the non-haemin iron in the human brain. *J Neurochem* 1958;3:41–51
- Martin WW, Ye FQ, Allen PS. Increasing striatal iron content associated with normal aging. *Mov Disord* 1998;13:281–86
- Drayer BP, Olanow W, Burger P, et al. Parkinson plus syndrome: diagnosis using high field MR imaging of brain iron. *Radiology* 1986;159:493–98
- Martin WR, Roberts TE, Ye FQ, et al. Increased basal ganglia iron in striatonigral degeneration: in vivo estimation with magnetic resonance. *Can J Neurol Sci* 1998;25:44–47
- Vymazal J, Righini A, Brooks RA, et al. T1 and T2 in the brain of healthy subjects, patients with Parkinson disease and patients with multiple system atrophy: relation to iron content. *Radiology* 1999;211:489–95
- Kraft E, Schwarz J, Trenkwalder C, et al. The combination of hypointense and hyperintense signal changes on T2-weighted magnetic resonance imaging sequences: a specific marker of multiple system atrophy? *Arch Neurol* 1999;56:225–28
- Kraft E, Trenkwalder C, Auer DP. T2*-weighted MRI differentiates multiple system atrophy from Parkinson's disease. *Neurology* 2002;59:1256–67
- Haller S, Badoud S, Nguyen D, et al. Differentiation between Parkinson disease and other forms of Parkinsonism using support vector machine analysis of susceptibility-weighted imaging (SWI): initial results. *Eur Radiol* 2013;23:12–19
- Collins SJ, Ahlskog JE, Parisi JE, et al. Progressive supranuclear palsy: neuropathologically based diagnostic clinical criteria. *J Neurol Neurosurg Psychiatry* 1995;58:167–73
- Nandigam RN, Viswanathan A, Delgado P, et al. MR imaging detection of cerebral microbleeds: effect of susceptibility-weighted imaging, section thickness, and field strength. *AJNR Am J Neuroradiol* 2009;30:338–43
- Wardlaw JM, Brindle W, Casado AM, et al. A systematic review of the utility of 1.5 versus 3 Tesla magnetic resonance brain imaging in clinical practice and research. *Eur Radiol* 2012;22:2295–303
- Martin WR, Wieler M, Gee M. Midbrain iron content in early Parkinson disease: a potential biomarker of disease status. *Neurology* 2008;70:1411–17
- Rossi ME, Ruottinen H, Saunamäki T, et al. Imaging brain iron and diffusion patterns: a follow-up study of Parkinson's disease in the initial stages. *Acad Radiol* 2014;21:64–71
- Blazejewska AI, Schwarz ST, Pitiot A, et al. Visualization of nigrosome 1 and its loss in PD: pathoanatomical correlation and in vivo 7 T MRI. *Neurology* 2013;81:534–40
- Kwon DH, Kim JM, Oh SH, et al. Seven-Tesla magnetic resonance images of the substantia nigra in Parkinson disease. *Ann Neurol* 2012;71:267–77
- Schwarz ST, Afzal M, Morgan PS, et al. The 'swallow tail' appearance of the healthy nigrosome: a new accurate test of Parkinson's disease—a case-control and retrospective cross-sectional MRI study at 3T. *PLoS One* 2014;9:e93814
- Hughes AJ, Daniel SE, Ben Shlomo Y, et al. The accuracy of diagnosis of parkinsonian syndromes in a specialist movement disorder service. *Brain* 2002;125:861–70